

PALI-3 VISION LANGUAGE MODELS: SMALLER, FASTER, STRONGER

Xi Chen^{*}₁ Xiao Wang^{*}₂ Lucas Beyer^{*}₂ Alexander Kolesnikov₂ Jialin Wu₁
 Paul Voigtlaender₁ Basil Mustafa₂ Sebastian Goodman₁ Ibrahim Alabdulmohsin₂
 Piotr Padlewski₂ Daniel Salz₁ Xi Xiong₃ Daniel Vlasic₃ Filip Pavetic₂
 Keran Rong₂ Tianli Yu₃ Daniel Keysers₂ Xiaohua Zhai^{*}₂[†] Radu Soricut[†]₁

¹Google Research ²Google DeepMind ³Google Cloud

ABSTRACT

This paper presents PaLI-3, a smaller, faster and stronger vision language model (VLM) that compares favorably to similar models that are 10x larger. As part of arriving at this strong performance, we compare Vision Transformer (ViT) models pretrained using classification objectives to contrastively pretrained ones (SigLIP). We find that, while slightly underperforming on standard image classification benchmarks, SigLIP-based PaLI shows superior performance across various multimodal benchmarks, especially on localization and text understanding. The SigLIP encoder we use is a scaled-up version using 2 billion parameters, and achieves a new state-of-the-art on multilingual cross-modal retrieval. We consider that PaLI-3, at only 5B parameters, rekindles research on fundamental pieces of complex VLMs, and could fuel a new generation of scaled-up models.

1 INTRODUCTION

The scaling of vision-language models (VLM) to tens and even hundreds of billions of parameters (Chen et al., 2023b; Alayrac et al., 2022; Chen et al., 2023a; Driess et al., 2023) has shown ever-increasing performance. Meanwhile, models at a smaller scale remain critical, as they are more practical to train and serve, more environmentally-friendly, and support faster research cycles for model design.

In the spirit of focusing on smaller-scale modeling, we present PaLI-3, the third-generation family of PaLI (Chen et al., 2023b) models. Using a pretrained backbone with only 5B total parameters, we refine the training recipe and achieve competitive and new state-of-the-art (SOTA) results on various VLM benchmarks. Our new recipe has three main components: contrastive pretraining of image encoder on web-scale image-text data (Zhai et al., 2023), an improved dataset mixture for PaLI multimodal training, and training at higher resolutions.

PaLI-3 achieves new SOTA results on tasks that require visually-situated text understanding and object localization, including eight visually-situated text understanding tasks and the referring expression segmentation task on RefCOCO (Yu et al., 2016), along with strong performance on a wide range of classical vision tasks. As part of this work, we also introduce a SOTA multilingual contrastive vision model scaled to 2B parameters, obtained using the recently-introduced SigLIP recipe (Zhai et al., 2023). Additionally, we perform focused ablation studies to compare the classification pretrained Vision Transformer (ViT) backbones (Dosovitskiy et al., 2021) with contrastively pretrained ones (SigLIP). This further confirms the viability of pretraining visual encoders on noisy web-scale image-text data, as a preferable alternative to training on classification-style data.

Our contributions are summarized as follows:

^{*}Core contributors, [†]Project leads

1. We compare classification pretrained ViT models (Dosovitskiy et al., 2021) to contrastively pretrained SigLIP models using the PaLI framework (Chen et al., 2023b). We find that the contrastively pretrained models work significantly better for visually-situated text understanding tasks and localization tasks.
2. Our model achieves SOTA performance on 10+ diverse vision-language benchmarks while being 10x smaller in size compared to the current SOTA model Chen et al. (2023a). For understanding visually-situated text, the improvement is by a particularly large margin.
3. Despite not pretraining on any video data, our model achieves new SOTA on several video QA benchmarks, indicative of powerful generalization abilities.
4. We introduce the 2 billion parameter (ViT-G) multilingual SigLIP model trained on WebLI (Chen et al., 2023b), which sets a new state-of-the-art on the multilingual cross-modal retrieval benchmark Thapliyal et al. (2022) across 36 languages.

2 RELATED WORK

Recent large vision language models (VLMs) use pretrained image encoders as part of the larger model, some pretrain it with supervised classification (PaLI (Chen et al., 2023b), PaLI-X (Chen et al., 2023a), Flamingo (Alayrac et al., 2022), PaLM-E (Driess et al., 2023)), some use pretrained CLIP encoders (BLIPv2 (Li et al., 2023), CrossTVR (Dai et al., 2023), ChatBridge (Zhao et al., 2023)) and some with custom multimodal pretraining (BEiT3 (Wang et al., 2022b), CoCa (Yu et al., 2022), SimVLM (Wang et al., 2021b)). In this paper we compare two dominant ways to pretrain image encoders using the PaLI framework: classification pretraining using large weakly labeled datasets (JFT, as in Kolesnikov et al., 2020; Zhai et al., 2022a; Dehghani et al., 2023) and contrastive pretraining on web-scale noisy data (WebLI, as in Zhai et al., 2023).

A recent finding spanning across PaLI (Chen et al., 2023b) and PaLI-X (Chen et al., 2023a) is that scaling up the classification pretrained image encoder seems more promising than was previously believed (Alayrac et al., 2022). Specifically, while classic image-only benchmarks such as ImageNet seem to indicate saturating performance from scaling pretraining of image-only models (Zhai et al., 2022a), PaLI shows that by scaling up the vision encoder from ViT-G (2B) to ViT-e (4B), the improvements on VL tasks are more noticeable than on ImageNet. PaLI-X further scaled up both the vision and language components, showing that these larger image encoders keep bringing benefit when plugged into large VLMs. This finding suggests that there is more to be found regarding the pretraining of image encoders in the context of VLMs, which may lead to different conclusions when looking at VLM tasks as compared to of “pure” vision tasks. In this paper, we dive into the impact of the image encoder for VLMs, by directly comparing classification pretrained vision models to contrastively pretrained ones, and reveal that the latter are vastly superior on a variety of tasks, especially localization and visually-situated text understanding.

One can split multimodal understanding capabilities into largely two categories: natural scene understanding (captioning, VQA, object detection/localization), and visually-situated text understanding (document and infographics QA). These groups of tasks require different granularity of understanding, and previous VLMs have largely focused on one type of tasks, leading to their training recipes being attuned to that type of tasks. For example PaLI-17B (Chen et al., 2023b) and Pix2struct (Lee et al., 2022) showed strong performance only on one of the two categories, respectively. The recent PaLI-X (Chen et al., 2023a) achieves SOTA performance on both categories, based on an improved OCR-related training recipe, and a significantly larger 55B parameter model. In this work, we combine the advantage of contrastively-pretrained ViT and a further improved and balanced training recipe into PaLI-3, and demonstrate that SOTA level performance on both the above categories of multimodal understanding is achievable even at 5B parameter scale.

3 MODEL

3.1 ARCHITECTURE

On a high level, the architecture follows Chen et al. (2023b;a): a ViT encodes the image into tokens which, together with text input (the question, prompt, instruction), are passed to an encoder-decoder transformer (Vaswani et al., 2017) that generates a text output.

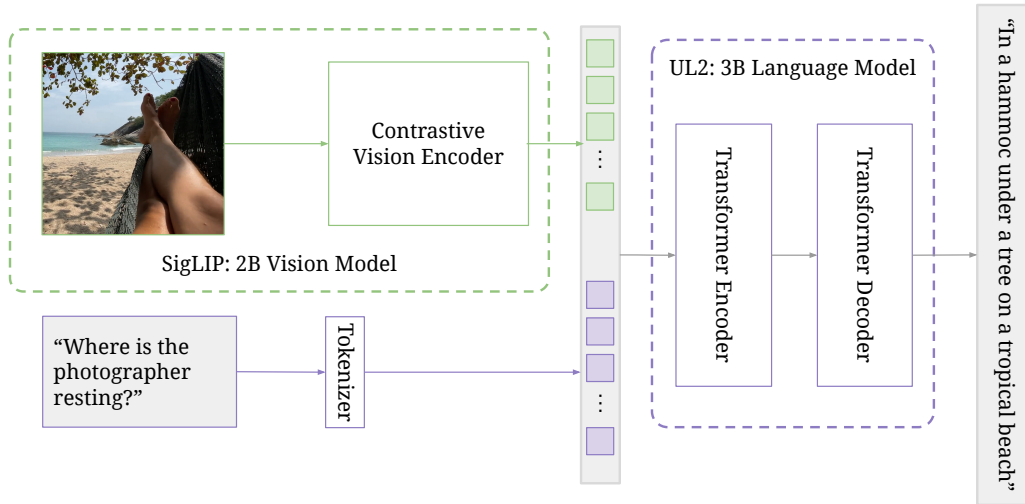


Figure 1: Overview of the PaLI-3 (5B) model: images are encoded into visual tokens individually by the contrastively pretrained 2B SigLIP vision model. Along with a query, these visual tokens are passed to an 3B encoder-decoder UL2 Transformer which produces the desired answer. In such a setup, a contrastively pretrained model provides significantly more useful tokens than one classification pretrained model as in previous PaLI models.

Visual component The vision backbone of PaLI-3 is initialized from a contrastively pretrained ViT-G/14² (Zhai et al., 2022a) model (approx. 2B parameters) using the SigLIP (Zhai et al., 2023) training recipe. In short, an image embedding ViT-G/14 and a text embedding transformer are trained to separately embed images and texts, such that a binary classifier using the sigmoid cross-entropy of the dot product of image and text embeddings correctly classifies whether the respective image and text correspond to each other or not. This is similar to CLIP (Radford et al., 2021) and ALIGN (Jia et al., 2021), but was shown to be more efficient, scalable, and robust (Zhai et al., 2023). This is done in order to pretrain the ViT image embedding component, hence the text embedding transformer is discarded when inserting the ViT into PaLI.

Full PaLI model The outputs of the ViT image encoder before pooling form the visual tokens, which are linearly projected and prepended to the embedded input text tokens. Together, these tokens are passed into a pretrained 3B parameter UL2 encoder-decoder language model (Tay et al., 2023), which generates text output. The text input to the model typically consists of a prompt that describes the type of task (e.g., “Generate the *alt_text* in $\langle \text{lang} \rangle$ at $\langle \text{pos} \rangle$ ” for captioning tasks) and encode necessary textual input for the task (e.g., “Answer in $\langle \text{lang} \rangle$: $\{ \text{question} \}$ ” for VQA tasks).

3.2 STAGES OF TRAINING

The training procedure is similar to that of PaLI and PaLI-X and consists of multiple stages:

Stage 0: Unimodal pretraining. The image encoder is pretrained contrastively on image-text pairs from the web, following the SigLIP training protocol (Zhai et al., 2023). This differs from PaLI and PaLI-X, where a JFT classification pretrained encoder was used. We use a model-based filtering approach similar to that in Schuhmann et al. (2021) that retains about 40% of the pairs. The image encoder is trained at resolution 224×224. The text encoder-decoder is a 3B UL2 model trained following the mixture of denoisers procedure described by Tay et al. (2023).

Stage 1: Multimodal training. Here, the image encoder is combined with the text encoder-decoder as described earlier and in Figure 1. Then, this combined PaLI model is trained on a multimodal task and data mixture, albeit keeping the image encoder *frozen* and using its native

²The embedding dimension was changed from 1664 to 1536 for better hardware utilization.

Table 1: Performance comparison between contrastively pre-trained (“SigLIP”) models and classification pre-trained (“Classif”) ViT image encoders using the same PaLI setup, across a wide range of tasks. While linear classification few-shot probing (first column) suggests SigLIP encoders are worse across many tasks, when plugged into PaLI and transferred, they show clear improvements. On the most complicated and detailed image understanding tasks, SigLIP models outperform Classif models by a large margin. Captioning numbers are CIDEr scores, where XM3600 shows the English performance in the first column, and the average across other languages in the second column. RefCOCO numbers are mIoU scores (details in Section 4.3).

		Probe	Captioning		VQA			RefCOCO			
		8 tasks	COCO	XM3600	v2	OK	Text	val	+	g	
G/14	Classif	88.1	139.9	94.5	44.7	76.7	57.2	31.9	51.6	43.5	43.4
	SigLIP	-2.5	+0.4	+1.6	+0.7	+0.8	+1.4	+18.7	+15.1	+19.1	+17.7
L/16	Classif	86.2	132.6	93.0	42.3	73.7	55.6	24.9	46.9	38.8	38.8
	SigLIP	-2.8	+3.2	+1.4	+1.4	+1.9	+1.9	+16.2	+17.4	+20.9	+20.1
B/16	Classif	83.7	127.7	91.7	40.7	72.3	54.7	22.5	46.3	38.1	38.4
	SigLIP	-2.6	+3.6	-2.0	-0.2	+1.4	+0.9	+13.3	+16.8	+19.6	+19.3

(224×224) resolution. The main mixture component is again derived from the WebLI dataset by heuristic filtering of the text quality and using the SplitCap training objective (Chen et al., 2023b). Further ingredients inherited from (Chen et al., 2023b) are multilingual captioning on CC3M-35L and WebLI OCR, cross-lingual VQA and VQG using VQ²A-CC3M-35L, object-aware VQA, as well as object detection. Notably, we do not include task or data derived from video (this was done in PaLI-X), but PaLI-3 retains competitive performance on these benchmarks thanks to its strong image encoder. We do, however, further improve document and text understanding capabilities by enriching WebLI with PDF documents with dense text and web-images described as posters or documents, in over 100 languages.

Stage 2: Resolution increase. High-resolution input is a widely accepted way of increasing performance, both due to making more details from the image perceptible, and due to increasing model power via increased sequence length. We increase PaLI-3’s resolution by fine-tuning the whole model (unfreezing the image encoder) with a short curriculum of increasing resolutions, keeping checkpoints at 812×812 and 1064×1064 resolution. The data mixture focuses on the part that involves visually-situated text and object detection.

Task specialization (transfer). Finally, for each individual task (benchmark), we fine-tune the PaLI-3 model with frozen ViT image encoder on the task’s training data as described in the corresponding section. For most tasks, we fine-tune the 812×812 resolution checkpoint, but for two document understanding tasks, we go up to 1064×1064 resolution.

4 EXPERIMENTS

4.1 CLASSIFICATION OR CONTRASTIVELY PRETRAINED ViT?

We first perform a controlled comparison of different ViT models within the PaLI framework. We consider two types of ViT models: classification pretrained (“Classif”) on the JFT dataset and contrastively pretrained on the WebLI dataset (“SigLIP”). We perform these experiments using a fixed 224×224 resolution (i.e. only include Stage 1) to save compute. We further shorten the Stage 1 phase to 20% of the full PaLI-3 schedule used in the remainder of this paper.

The results in Table 1 paint a clear picture overall: While the few-shot linear classification (Dosovitskiy et al., 2021) of SigLIP models falls behind, when used in PaLI-3, SigLIP models provide moderate gains on “simpler” tasks such as captioning and question-answering, and large gains for more “complicated” scene-text and spatial understanding tasks such as TextVQA and RefCOCO

Table 2: Results on benchmarks more focused on understanding visually-situated text. TextCaps, TextVQA, STVQA, InfographicVQA and DocVQA are all evaluated using the corresponding official evaluation server. Methods marked by "†" are trained on additional VQA data similar to the target benchmark, before finetuning on the target benchmark. For ChartQA, we compare with similar setups by finetuning without chain-of-thought or similar prompting techniques. The SOTA models are (a) Chen et al. (2023a), (b) Powalski et al. (2021), (c) Peng et al. (2022).

Model	Text Caps	Text VQA	ST VQA	OCR VQA	Info VQA	Doc VQA	AI2D	Chart QA	Screen2 Words	Widget Cap	Avg. of first 8
<i>with OCR pipeline input</i>											
SOTA	163.7 (a)	80.78 (a)	84.5 (a)	77.3 (a)	61.2 (b)†	88.4 (c)†	81.4 (a)	72.3 (a)	-	-	88.7
PaLI-3	164.3	80.78	85.7	77.8	62.4	88.6	75.2	69.5	-	-	88.0 (-0.7)
<i>without OCR pipeline input</i>											
SOTA	147.0 (a)	71.44 (a)	79.9 (a)	75.0 (a)	49.2 (a)	80.0 (a)	81.2 (a)	70.9 (a)	127.9 (a)	153.0 (a)	81.8
PaLI-3	158.8	79.51	84.1	76.7	57.8	87.6	75.2	70.0	130.7	159.8	86.2 (+4.4)

variants. This motivates the departure from classification pretrained image encoders, and switching to sigmoid-contrastively pretrained ones for building PaLI-3.

4.2 VISUALLY-SITUATED TEXT UNDERSTANDING

We evaluate PaLI-3 on visually-situated text understanding tasks: TextCaps (Sidorov et al., 2020), TextVQA (Singh et al., 2019), STVQA (Biten et al., 2019), OCRVQA (Mishra et al., 2019), InfographicVQA (Mathew et al., 2022), DocVQA (Mathew et al., 2021), ChartQA (Masry et al., 2022), Scree2Words (Wang et al., 2021a), and WidgetCap (Li et al., 2020). The images in those datasets span a wide range of domains such as natural images, illustrations, documents and user interfaces.

For the InfographicVQA and DocVQA benchmarks we fine-tune the 1064×1064 resolution model, all others use the 812×812 one. We report the standard metrics for each benchmark, namely: CIDEr score for all the Image Captioning benchmarks; VQA accuracy for VQAv2, OKVQA, and TextVQA; Average Normalized Levenshtein Similarity (ANLS) for ST-VQA, DocVQA and InfographicsVQA; Exact match (EM) for TallyQA, OCR-VQA and AI2D; Relaxed-Accuracy (RA) for ChartQA. For visually-situated text understanding, external OCR systems are usually leveraged to provide OCR annotations of the image as an additional input to the model for boosting performance. Here we follow (Chen et al., 2023a) and report the result of finetuning PaLI-3 both with and without OCR inputs. The OCR annotations are obtained using the same service as that for the training set. As shown in Table 2, PaLI-3 achieves SOTA performance on a vast majority of the captioning and VQA benchmarks both with and without external OCR input. The exception is AI2D and ChartQA, which require not just understanding but also strong reasoning capability over diagrams and charts, respectively. For these two benchmarks, PaLI-3 falls slightly behind PaLI-X (Chen et al., 2023a) likely due to the latter’s significantly larger 32B LLM being better at reasoning.

Averaging over the 8 benchmarks in Table 2 that have results in all settings, PaLI-3 is only 0.7 points behind all SOTA methods combined in the setting where external OCR systems are used. However, in the setting without such external system, PaLI-3 has a significant 4.4 point advantage over all SOTA methods combined. For TextCaps, TextVQA, InfographicVQA and DocVQA this advantage is 8 points or more. Finally, we can see that PaLI-3 without any external OCR system is only 1.8 points behind relying on one, suggesting the image encoder learns a strong intrinsic OCR capability.

4.3 REFERRING EXPRESSION SEGMENTATION

We extend PaLI-3 with the capability to predict segmentation masks via language-like output. To this end, we make use of the vector-quantized variational auto-encoder (VQ-VAE) from Ning et al. (2023). The VQ-VAE is trained to learn a discrete codebook of 128 mask tokens. Its encoder can

Table 3: PaLI referring expression segmentation results on RefCOCO (Yu et al., 2016) variants. All results are mIoU on the `val` split.

Model	RefCOCO	RefCOCO+	G-Ref
RefTr (Li & Sigal, 2021)	74.34	66.75	66.63
PolyFormer (Liu et al., 2023)	76.94	72.15	71.15
PaLI-3 (Ours)	77.33	73.53	72.72

tokenize a 64×64 pixels segmentation mask into 16 mask tokens, which its decoder can convert back. We train PaLI-3 to predict a single segmentation mask. First, PaLI-3 outputs 4 coordinates as text, representing a bounding box. This is followed by 16 mask tokens that represent the mask inside the bounding box.

We fine-tune PaLI-3 on the combined training sets of RefCOCO, RefCOCO+, and RefCOCOg (Yu et al., 2016)³ at 812×812 resolution. Each training example consists of a referring expression (e.g. “the large brown dog on the left”), and a box with segmentation mask. We prompt PaLI with the prompt “*detect: the large brown dog on the left* `<extra_id_0>`”, and the target is a sequence like “*348 543 684 664* `<mask_token_81>` ... `<mask_token_10>`”. The target sequence contains 16 mask tokens between 0 and 127 that are generated by the VQ-VAE encoder using the segmentation mask cropped and resized to 64×64 as input.

The results in Table 1 demonstrate that contrastive pretraining is much more effective than classification pretraining for localization task of this type. Table 3 shows that the full PaLI-3 model is able to slightly outperform the state of the art in referring expression segmentation.

4.4 NATURAL IMAGE UNDERSTANDING

In this section, we evaluate PaLI-3 on general vision-language understanding tasks, including COCO captions (Karpathy & Fei-Fei, 2015) and VQAv2 (Goyal et al., 2017) which target general visual understanding, OKVQA (Marino et al., 2019) which focuses on knowledge-based understanding and TallyQA (Acharya et al., 2019) which measures performance on counting under textual guidance. All results for the benchmarks presented in Table 4 use 812×812 resolution. As in previous work, they employ no external OCR module, since these benchmarks rarely involve text in the image.

Overall, PaLI-3 shows very strong performance on these benchmarks despite its significantly smaller size compared to recent SOTA models. For COCO, PaLI-3 outperforms all models but BEiT-3 and the 17B and 55B PaLI. On VQAv2 and TallyQA, PaLI-3 exceeds all previous models except PaLI-X, with a less than 1 point gap on VQAv2. For the knowledge-intensive OKVQA task, which usually benefits from a large language component, PaLI-3 is only behind PaLM-E (562B) and PaLI-X (55B) but still outperforms the 32-shot Flamingo (80B) model.

4.5 VIDEO CAPTIONING AND QUESTION ANSWERING

We fine-tune and evaluate the PaLI-3 model on 4 video captioning benchmarks: MSR-VTT (Xu et al., 2016), VATEX (Wang et al., 2019), ActivityNet Captions (Krishna et al., 2017), and Spoken Moments in Time (Monfort et al., 2021). We do the same for 3 video question-answering benchmarks: NExT-QA (Xiao et al., 2021), MSR-VTT-QA (Xu et al., 2017), and ActivityNet-QA (Yu et al., 2019). A brief description of each benchmark and its usage is provided in Appendix A.

Following the setup from PaLI-X (Chen et al., 2023a), we fine-tune our model using the Stage 1 checkpoint with 224×224 resolution for each task separately. We sample at most 16 frames with a fixed temporal stride for each benchmark. Each frame is independently processed by the ViT image encoder, the resulting visual tokens are simply concatenated, leading to up to 4096 visual tokens. A key difference from the PaLI-X setup is that there is no video data in PaLI-3 pretraining, meaning PaLI-3 has never seen multi-frame inputs during pretraining.

³We removed all validation and test images from the training set for both PaLI and the VQ-VAE

Table 4: Results on COCO Captions (Karpathy split), VQAv2, OKVQA, and TallyQA. (*Flamingo reports 32 shot result). Underscored numbers indicate that PaLI-3 is only behind the 55B PaLI-X and is better than all other models in the list.

Model	COCO	VQAv2		OKVQA	TallyQA	
	Karp.-test	test-dev	test-std	val	Simple	Complex
SimVLM	143.3	80.03	80.34	-	-	-
CoCa (2.1B)	143.6	82.3	82.3	-	-	-
GIT (0.7B)	144.8	78.56	78.81	-	-	-
GIT2 (5.1B)	145.0	81.74	81.92	-	-	-
OFA (0.9B)	145.3	82.0	82.0	-	-	-
Flamingo (80B)	138.1	82.0	82.1	57.8*	-	-
BEiT-3 (1.9B)	147.6	84.2	84.0	-	-	-
PaLM-E (562B)	138.7	80.0	-	66.1	-	-
MoVie	-	69.26	-	-	74.9	56.8
PaLI-17B	149.1	84.3	84.3	64.5	81.7	70.9
PaLI-X (55B)	149.2	86.0	86.1	66.1	86.0	75.6
PaLI-3 (5B)	145.9	<u>85.0</u>	<u>85.2</u>	60.1	<u>83.3</u>	70.5

Table 5: Results for Video Captioning and Video-QA using up to 16 frames. †GIT2 directly optimizes the CIDEr metric. mPLUG-2 is Xu et al. (2023), PaLI-X is Chen et al. (2023a), GIT2 is Wang et al. (2022a), and Flamingo-32 is the 32-shot variant of Alayrac et al. (2022).

Method	MSR-VTT		Activity-Net		VATEX	SMIT	NExT-QA
	Caption	QA	Caption	QA	Caption	Caption	QA
Prior SOTA	80.3	48.0	54.9	49.4	94.0 [†]	43.5	38.3
	mPLUG-2	mPLUG-2	PaLI-X	PaLI-X	GIT2	PaLI-X	Flamingo-32
PaLI-3	78.3	49.3	50.8	51.2	66.9	39.6	37.7

Despite not being pretrained with video data, PaLI-3 achieves excellent video QA results with a small model size: a new state of the art performance on MSR-VTT-QA and ActivityNet-QA, and competitive results on NextQA. The consistent improvements on image and video QA highlight the benefits of adopting the contrastive ViTs. PaLI-3 also achieves respectable video captioning results, under-performing the SOTA by only 3 CIDEr points on average. Considering the model size, PaLI-3 appears to be an excellent choice in terms of both performance and practicality.

Table 6: Evaluations of the visual component in isolation (without the language model). We report fine-tuned classification accuracy on ImageNet, ImageNet-ReaL and ImageNet-V2; average zero-shot cross-modal retrieval recall@1 across 36 languages on XM3600; average 10-shot linear probe classification accuracy across 8 tasks.

Model	Encoder	ImageNet (fine-tuning)				XM3600 (retrieval)		Probe
		Res.	Val	ReaL	v2	I→T	T→I	8 tasks
PaLI-3	SigLIP ViT-G	518px	89.6	90.9	82.3	56.9	44.0	85.6
PaLI-15B	Classif ViT-G	518px	90.5	90.8	83.3	-	-	88.1
PaLI-17B	Classif ViT-e	644px	90.9	91.1	84.3	36.0	28.5	89.5
PaLI-X	Classif ViT-22B	756px	89.2	91.0	83.7	-	-	89.9

Table 7: RAI statistics for captions generated by PaLI-3 on FairFace (Karkkainen & Joo, 2021).

	Perceived Gender		Ethnicity			Age Bucket			Overall
	Lowest	Highest	Lowest	Median	Highest	Lowest	Median	Highest	
Toxicity	0.02%	0.05%	0.00%	0.00%	0.10%	0.00%	0.00%	0.07%	0.04%
Profanity	0.00%	0.00%	0.00%	0.00%	0.00%	0.00%	0.00%	0.00%	0.00%
Insult	0.04%	0.10%	0.00%	0.07%	0.14%	0.00%	0.06%	0.17%	0.07%
Threat	0.10%	0.12%	0.00%	0.14%	0.20%	0.00%	0.00%	0.21%	0.11%
Attack	0.00%	0.00%	0.00%	0.00%	0.00%	0.00%	0.00%	0.00%	0.00%

Table 8: RAI score statistics in the captions generated by PaLI-3 on MIAP (Schumann et al., 2021).

	Perceived Gender		Age Bucket			Skin Tone			Overall
	Lowest	Highest	Lowest	Median	Highest	Lowest	Median	Highest	
Toxicity	0.05%	0.10%	0.05%	0.24%	0.48%	0.00%	0.00%	0.26%	0.07%
Profanity	0.10%	0.10%	0.00%	0.12%	0.24%	0.00%	0.00%	0.10%	0.10%
Insult	0.10%	0.14%	0.00%	0.13%	0.17%	0.00%	0.00%	0.38%	0.13%
Threat	0.34%	0.80%	0.30%	0.54%	1.68%	0.00%	0.59%	0.94%	0.65%
Identity Attack	0.00%	0.00%	0.00%	0.00%	0.00%	0.00%	0.00%	0.00%	0.00%

4.6 DIRECT IMAGE ENCODER EVALUATION

Here, we aim to directly evaluate the learned image encoder (ViT-G model) without the surrounding language model, i.e. not the full PaLI-3. All results are summarized in Table 6.

First, we test image classification capabilities using the standard ImageNet (Russakovsky et al., 2014) benchmark and two of its most popular variants (Beyer et al., 2020; Recht et al., 2019). We fine-tune the unimodal image encoder from Stage 0 on ImageNet and compare it to fine-tuning of classification pretrained ViTs used in previous PaLI models. The main comparison is to the classification (Classif) pretrained ViT-G/14 model from Zhai et al. (2022a). The SigLIP slightly lags behind in terms of top-1 and v2 accuracy, but matches in terms of Real accuracy (Beyer et al., 2020), a metric which avoids measuring “overfitting” to ImageNet peculiarities.

Second, we report multilingual image-text retrieval results on the Crossmodal-3600 benchmark (Thapliyal et al., 2022). Since classification pretrained image encoders do not have this capability, we LiT-tune (Zhai et al., 2022b) a text encoder for it on the multilingual WebLI dataset. We also LiT-tune a new text encoder for the SigLIP image encoder in the exact same setting, to remove any confounders from the comparison. The SigLIP ViT-G model clearly outperforms the classification pretrained larger ViT-e model.

Finally, we perform linear probing of the representation in the few-shot setting following Dosovitskiy et al. (2021); Zhai et al. (2022a) across the 8 different classification tasks also used in Zhai et al. (2022a) and report the average performance. Here, we see that SigLIP lags behind, likely because the representation is not pretrained in a way that supports linear separability, as was recently uncovered by Tschannen et al. (2023).

Taken together, these results paint a clear picture: the best and largest classification pretrained image encoders appear (slightly) better when evaluated on standard classification tasks, however they are significantly worse than SigLIP pretrained image encoders for vision-language tasks.

5 MODEL FAIRNESS, BIASES, AND OTHER POTENTIAL ISSUES

We follow the evaluation protocol of Chen et al. (2023a) to assess the model fairness, biases, and other potential issues. First, we use the MIAP (Schumann et al., 2021) and FairFace (Karkkainen & Joo, 2021) datasets to generate captions and use the Perspective API (Lees et al., 2022) (threshold > 0.8) to measure toxicity and profanity among other potential issues. Table 7 (FairFace) and Table 8 (MIAP) summarize the results. Slices with < 20 examples are dropped from the analysis. Overall, we observe a low level of toxicity and profanity among others, across all slices. The results are comparable to those in PaLI-X (Chen et al., 2023a).

Table 9: Detection error rate for “person” in PaLI-3 using the subset of the MIAP dataset (Schumann et al., 2021) that contain exactly a single individual in the image. PaLI-3 maintains a low error rate across all subgroups. Skin tone follows the Monk Skin Tone Scale (Monk, 2019). Numbers inside square brackets correspond to the size of each bucket.

Skin Tone	1 [2]	2 [871]	3 [3008]	4 [522]	5 [184]	6 [85]	7 [54]	8 [49]	9 [6]	10 [1]
	0.00%	0.00%	0.17%	0.39%	0.00%	0.00%	0.00%	0.00%	0.00%	0.00%
Gender	Predominantly Feminine [2437]					Predominantly Masculine [3544]				
	0.41%					1.78%				
Age Bucket	0-2 yrs [17]		3-19 yrs [568]		20-59 yrs [4925]		> 60 yrs [247]			
	0.00%		0.18%		1.30%		0.82%			

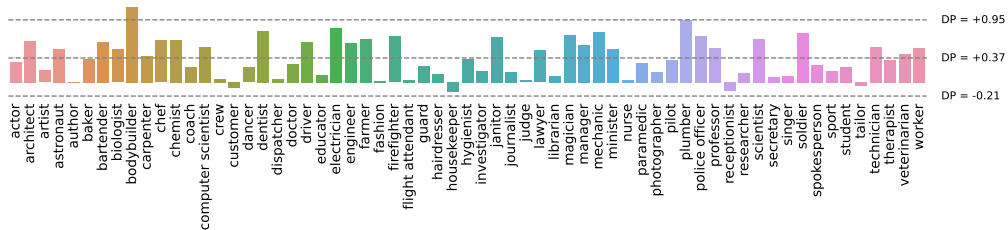


Figure 2: Level of demographic parity (DP) in PaLI-3’s output for CelebA images, comparing the average log-perplexity between females and males. Values close to zero indicate absence of bias. The dotted lines correspond to μ and $\mu \pm 2\sigma$. DP for all occupations falls within the 95% confidence interval, except “bodybuilder” and “plumber” which the model tends to strongly associate with men.

Second, we examine the level of demographic parity (Dwork et al., 2012) in the model itself. Following (Chen et al., 2023a), we feed an image from the CelebA dataset (Liu et al., 2015) into PaLI-3 with the chosen occupation as a prefix and record the average log-perplexity score of the model generation. The demographic parity is the difference between average log-perplexity within the demographic groups. Figure 2 summarizes the results: Similar to PaLI-X, PaLI-3 tends to assign a *higher* log-perplexity score to women than men across most occupations with a mean difference of $\mu = 0.37$. However, fewer occupations in PaLI-3 fall outside the interval $\mu \pm 2\sigma$ compared to PaLI-X.

Third, we compare performance across all subgroups on a detection task using the MIAP dataset, following again (Chen et al., 2023a). For images containing exactly a single individual, we query PaLI-3 with the question: “Is there a person in this image?” and evaluate the accuracy of its response. Table 9 summarizes the results. The error rate (false negatives) is very low across all subgroups.

For analysis of the WebLI dataset itself, such as the correlations between perceived gender and occupations, see Chen et al. (2023a).

Limitations. The limitations of this work are very similar to those already presented in the literature. We refer to (Chen et al., 2023a), which raises all limitations that apply to our work.

6 CONCLUSION

In this paper, we took a closer look at the pretraining of the image encoder in large VLMs, specifically the PaLI type of model. By performing controlled experiments on that part, for the first time, we clearly compare the two camps of classification pretraining and image-text (contrastive) pretraining, finding that the latter can lead to better and more efficient VLMs, especially for localization and text understanding tasks. This is just *one small aspect* of VLMs, and we hope this study and result spurs to further detailed investigations of the *many other aspects* of training VLMs.

7 ACKNOWLEDGEMENTS

We would like to thank Bo Pang, Michael Tschannen, Soravit Changpinyo, AJ Piergiovanni, Marvin Ritter, Yi Tay, Paulina Pietrzyk, Matthias Minderer, André Susano Pinto, Mojtaba Seyedhosseini, Anelia Angelova, Neil Houlsby, Yiming Gu, Daniel Hernandez Diaz, Chun-Liang Li, Guolong Su, Hao Zhang, Chenxia Wu, Rui Lin, Ting Yu, Weina Ge, Shengyang Dai, Tania Bedrax-Weiss, Rob Fergus and Joelle Barral for helpful discussions, feedback, and support. We thank the Google Research and Google DeepMind groups for providing a fruitful environment to conduct research.

REFERENCES

- Manoj Acharya, Kushal Kafle, and Christopher Kanan. Tallyqa: Answering complex counting questions. In *The Thirty-Third AAAI Conference on Artificial Intelligence, AAAI 2019, The Thirty-First Innovative Applications of Artificial Intelligence Conference, IAAI 2019, The Ninth AAAI Symposium on Educational Advances in Artificial Intelligence, EAAI 2019, Honolulu, Hawaii, USA, January 27 - February 1, 2019*, pp. 8076–8084. AAAI Press, 2019. doi: 10.1609/aaai.v33i01.33018076. URL <https://doi.org/10.1609/aaai.v33i01.33018076>.
- Jean-Baptiste Alayrac, Jeff Donahue, Pauline Luc, Antoine Miech, Iain Barr, Yana Hasson, Karel Lenc, Arthur Mensch, Katie Millican, Malcolm Reynolds, et al. Flamingo: a visual language model for few-shot learning. *arXiv preprint arXiv:2204.14198*, 2022.
- Lucas Beyer, Olivier J Hénaff, Alexander Kolesnikov, Xiaohua Zhai, and Aäron van den Oord. Are we done with ImageNet? *arXiv preprint arXiv:2006.07159*, 2020.
- Ali Furkan Biten, Ruben Tito, Andres Mafla, Lluís Gomez, Marçal Rusinol, Ernest Valveny, CV Jawahar, and Dimosthenis Karatzas. Scene text visual question answering. In *Proceedings of the IEEE/CVF international conference on computer vision*, pp. 4291–4301, 2019.
- Xi Chen, Josip Djolonga, Piotr Padlewski, Basil Mustafa, Soravit Changpinyo, Jialin Wu, Carlos Riquelme Ruiz, Sebastian Goodman, Xiao Wang, Yi Tay, Siamak Shakeri, Mostafa Dehghani, Daniel Salz, Mario Lucic, Michael Tschannen, Arsha Nagrani, Hexiang Hu, Mandar Joshi, Bo Pang, Ceslee Montgomery, Paulina Pietrzyk, Marvin Ritter, AJ Piergiovanni, Matthias Minderer, Filip Pavetic, Austin Waters, Gang Li, Ibrahim Alabdulmohsin, Lucas Beyer, Julien Amelot, Kenton Lee, Andreas Peter Steiner, Yang Li, Daniel Keysers, Anurag Arnab, Yuanzhong Xu, Keran Rong, Alexander Kolesnikov, Mojtaba Seyedhosseini, Anelia Angelova, Xiaohua Zhai, Neil Houlsby, and Radu Soricut. Pali-x: On scaling up a multilingual vision and language model, 2023a.
- Xi Chen, Xiao Wang, Soravit Changpinyo, AJ Piergiovanni, Piotr Padlewski, Daniel Salz, Sebastian Alexander Goodman, Adam Grycner, Basil Mustafa, Lucas Beyer, Alexander Kolesnikov, Joan Puigcerver, Nan Ding, Keran Rong, Hassan Akbari, Gaurav Mishra, Linting Xue, Ashish Thapliyal, James Bradbury, Weicheng Kuo, Mojtaba Seyedhosseini, Chao Jia, Burcu Karagol Ayan, Carlos Riquelme, Andreas Steiner, Anelia Angelova, Xiaohua Zhai, Neil Houlsby, and Radu Soricut. PaLI: A jointly-scaled multilingual language-image model. In *ICLR*, 2023b.
- Zuozhuo Dai, Fangtao Shao, Qingkun Su, Zilong Dong, and Siyu Zhu. Fine-grained text-video retrieval with frozen image encoders. *CoRR*, abs/2307.09972, 2023. doi: 10.48550/arXiv.2307.09972. URL <https://doi.org/10.48550/arXiv.2307.09972>.
- Mostafa Dehghani, Josip Djolonga, Basil Mustafa, Piotr Padlewski, Jonathan Heek, Justin Gilmer, Andreas Steiner, Mathilde Caron, Robert Geirhos, Ibrahim Alabdulmohsin, Rodolphe Jenatton, Lucas Beyer, Michael Tschannen, Anurag Arnab, Xiao Wang, Carlos Riquelme, Matthias Minderer, Joan Puigcerver, Utku Evci, Manoj Kumar, Sjoerd van Steenkiste, Gamaleldin F. Elsayed, Aravindh Mahendran, Fisher Yu, Avital Oliver, Fantine Huot, Jasmijn Bastings, Mark Patrick Collier, Alexey Gritsenko, Vighnesh Birodkar, Cristina Vasconcelos, Yi Tay, Thomas Mensink, Alexander Kolesnikov, Filip Pavetić, Dustin Tran, Thomas Kipf, Mario Lučić, Xiaohua Zhai, Daniel Keysers, Jeremiah Harmsen, and Neil Houlsby. Scaling vision transformers to 22 billion parameters, 2023. URL <https://arxiv.org/abs/2302.05442>.

- Alexey Dosovitskiy, Lucas Beyer, Alexander Kolesnikov, Dirk Weissenborn, Xiaohua Zhai, Thomas Unterthiner, Mostafa Dehghani, Matthias Minderer, Georg Heigold, Sylvain Gelly, Jakob Uszkoreit, and Neil Houlsby. An image is worth 16x16 words: Transformers for image recognition at scale. In *9th International Conference on Learning Representations, ICLR 2021, Virtual Event, Austria, May 3-7, 2021*. OpenReview.net, 2021. URL <https://openreview.net/forum?id=YicbFdNTTy>.
- Danny Driess, Fei Xia, Mehdi S. M. Sajjadi, Corey Lynch, Aakanksha Chowdhery, Brian Ichter, Ayzan Wahid, Jonathan Tompson, Quan Vuong, Tianhe Yu, Wenlong Huang, Yevgen Chebotar, Pierre Sermanet, Daniel Duckworth, Sergey Levine, Vincent Vanhoucke, Karol Hausman, Marc Toussaint, Klaus Greff, Andy Zeng, Igor Mordatch, and Pete Florence. Palm-e: An embodied multimodal language model. In Andreas Krause, Emma Brunskill, Kyunghyun Cho, Barbara Engelhardt, Sivan Sabato, and Jonathan Scarlett (eds.), *International Conference on Machine Learning, ICML 2023, 23-29 July 2023, Honolulu, Hawaii, USA*, volume 202 of *Proceedings of Machine Learning Research*, pp. 8469–8488. PMLR, 2023. URL <https://proceedings.mlr.press/v202/driess23a.html>.
- Cynthia Dwork, Moritz Hardt, Toniann Pitassi, Omer Reingold, and Richard S. Zemel. Fairness through awareness. In Shafi Goldwasser (ed.), *Innovations in Theoretical Computer Science 2012, Cambridge, MA, USA, January 8-10, 2012*, pp. 214–226. ACM, 2012. doi: 10.1145/2090236.2090255. URL <https://doi.org/10.1145/2090236.2090255>.
- Yash Goyal, Tejas Khot, Douglas Summers-Stay, Dhruv Batra, and Devi Parikh. Making the V in VQA matter: Elevating the role of image understanding in visual question answering. In *Proceedings of the IEEE conference on computer vision and pattern recognition*, pp. 6904–6913, 2017.
- Chao Jia, Yinfei Yang, Ye Xia, Yi-Ting Chen, Zarana Parekh, Hieu Pham, Quoc V. Le, Yun-Hsuan Sung, Zhen Li, and Tom Duerig. Scaling up visual and vision-language representation learning with noisy text supervision. In Marina Meila and Tong Zhang (eds.), *Proceedings of the 38th International Conference on Machine Learning, ICML 2021, 18-24 July 2021, Virtual Event*, volume 139 of *Proceedings of Machine Learning Research*, pp. 4904–4916. PMLR, 2021. URL <http://proceedings.mlr.press/v139/jia21b.html>.
- Kimmo Karkkainen and Jungseock Joo. Fairface: Face attribute dataset for balanced race, gender, and age for bias measurement and mitigation. In *Proceedings of the IEEE/CVF Winter Conference on Applications of Computer Vision*, pp. 1548–1558, 2021.
- Andrej Karpathy and Li Fei-Fei. Deep visual-semantic alignments for generating image descriptions. In *CVPR*, 2015.
- Alexander Kolesnikov, Lucas Beyer, Xiaohua Zhai, Joan Puigcerver, Jessica Yung, Sylvain Gelly, and Neil Houlsby. Big transfer (bit): General visual representation learning. In Andrea Vedaldi, Horst Bischof, Thomas Brox, and Jan-Michael Frahm (eds.), *Computer Vision - ECCV 2020 - 16th European Conference, Glasgow, UK, August 23-28, 2020, Proceedings, Part V*, volume 12350 of *Lecture Notes in Computer Science*, pp. 491–507. Springer, 2020. doi: 10.1007/978-3-030-58558-7_29. URL https://doi.org/10.1007/978-3-030-58558-7_29.
- Ranjay Krishna, Kenji Hata, Frederic Ren, Li Fei-Fei, and Juan Carlos Niebles. Dense-captioning events in videos. In *Proceedings of the IEEE/CVF Conference on Computer Vision and Pattern Recognition*, 2017.
- Kenton Lee, Mandar Joshi, Iulia Turc, Hexiang Hu, Fangyu Liu, Julian Eisenschlos, Urvashi Khandelwal, Peter Shaw, Ming-Wei Chang, and Kristina Toutanova. Pix2struct: Screenshot parsing as pretraining for visual language understanding. *arXiv preprint arXiv:2210.03347*, 2022.
- Alyssa Lees, Vinh Q Tran, Yi Tay, Jeffrey Sorensen, Jai Gupta, Donald Metzler, and Lucy Vasserman. A new generation of perspective API: Efficient multilingual character-level transformers. *arXiv preprint arXiv:2202.11176*, 2022.

- Junnan Li, Dongxu Li, Silvio Savarese, and Steven C. H. Hoi. BLIP-2: bootstrapping language-image pre-training with frozen image encoders and large language models. In Andreas Krause, Emma Brunskill, Kyunghyun Cho, Barbara Engelhardt, Sivan Sabato, and Jonathan Scarlett (eds.), *International Conference on Machine Learning, ICML 2023, 23-29 July 2023, Honolulu, Hawaii, USA*, volume 202 of *Proceedings of Machine Learning Research*, pp. 19730–19742. PMLR, 2023. URL <https://proceedings.mlr.press/v202/li23q.html>.
- Muchen Li and Leonid Sigal. Referring transformer: A one-step approach to multi-task visual grounding. In Marc’Aurelio Ranzato, Alina Beygelzimer, Yann N. Dauphin, Percy Liang, and Jennifer Wortman Vaughan (eds.), *Advances in Neural Information Processing Systems 34: Annual Conference on Neural Information Processing Systems 2021, NeurIPS 2021, December 6-14, 2021, virtual*, pp. 19652–19664, 2021. URL <https://proceedings.neurips.cc/paper/2021/hash/a376802c0811f1b9088828288eb0d3f0-Abstract.html>.
- Yang Li, Gang Li, Luheng He, Jingjie Zheng, Hong Li, and Zhiwei Guan. Widget captioning: Generating natural language description for mobile user interface elements. In *Proceedings of the 2020 Conference on Empirical Methods in Natural Language Processing (EMNLP)*, pp. 5495–5510, Online, November 2020. Association for Computational Linguistics. doi: 10.18653/v1/2020.emnlp-main.443. URL <https://aclanthology.org/2020.emnlp-main.443>.
- Jiang Liu, Hui Ding, Zhaowei Cai, Yuting Zhang, Ravi Kumar Satzoda, Vijay Mahadevan, and R Manmatha. Polyformer: Referring image segmentation as sequential polygon generation. In *Proceedings of the IEEE/CVF Conference on Computer Vision and Pattern Recognition*, pp. 18653–18663, 2023.
- Ziwei Liu, Ping Luo, Xiaogang Wang, and Xiaoou Tang. Deep learning face attributes in the wild. In *International Conference on Computer Vision*, 2015.
- Kenneth Marino, Mohammad Rastegari, Ali Farhadi, and Roozbeh Mottaghi. OK-VQA: A visual question answering benchmark requiring external knowledge. In *Proceedings of the IEEE/cv conference on computer vision and pattern recognition*, pp. 3195–3204, 2019.
- Ahmed Masry, Do Long, Jia Qing Tan, Shafiq Joty, and Enamul Hoque. ChartQA: A benchmark for question answering about charts with visual and logical reasoning. In *Findings of ACL*, 2022.
- Minesh Mathew, Dimosthenis Karatzas, and CV Jawahar. Docvqa: A dataset for vqa on document images. In *Proceedings of the IEEE/CVF winter conference on applications of computer vision*, pp. 2200–2209, 2021.
- Minesh Mathew, Viraj Bagal, Rubèn Tito, Dimosthenis Karatzas, Ernest Valveny, and CV Jawahar. Infographicvqa. In *Proceedings of the IEEE/CVF Winter Conference on Applications of Computer Vision*, pp. 1697–1706, 2022.
- Anand Mishra, Shashank Shekhar, Ajeet Kumar Singh, and Anirban Chakraborty. Ocr-vqa: Visual question answering by reading text in images. In *ICDAR*, 2019.
- Mathew Monfort, SouYoung Jin, Alexander Liu, David Harwath, Rogerio Feris, James Glass, and Aude Oliva. Spoken moments: Learning joint audio-visual representations from video descriptions. In *Proceedings of the IEEE/CVF Conference on Computer Vision and Pattern Recognition*, pp. 14871–14881, 2021.
- Ellis Monk. Monk skin tone scale, 2019. URL <https://skintone.google>.
- Jia Ning, Chen Li, Zheng Zhang, Zigang Geng, Qi Dai, Kun He, and Han Hu. All in tokens: Unifying output space of visual tasks via soft token. *arXiv preprint arXiv:2301.02229*, 2023.
- Qiming Peng, Yinxu Pan, Wenjin Wang, Bin Luo, Zhenyu Zhang, Zhengjie Huang, Teng Hu, Weichong Yin, Yongfeng Chen, Yin Zhang, et al. Ernie-layout: Layout knowledge enhanced pre-training for visually-rich document understanding. *arXiv preprint arXiv:2210.06155*, 2022.
- Rafał Powalski, Łukasz Borchmann, Dawid Jurkiewicz, Tomasz Dwojak, Michał Pietruszka, and Gabriela Pałka. Going full-tilt boogie on document understanding with text-image-layout transformer. In *Document Analysis and Recognition—ICDAR 2021: 16th International Conference, Lausanne, Switzerland, September 5–10, 2021, Proceedings, Part II 16*, pp. 732–747. Springer, 2021.

- Alec Radford, Jong Wook Kim, Chris Hallacy, Aditya Ramesh, Gabriel Goh, Sandhini Agarwal, Girish Sastry, Amanda Askell, Pamela Mishkin, Jack Clark, Gretchen Krueger, and Ilya Sutskever. Learning transferable visual models from natural language supervision. In Marina Meila and Tong Zhang (eds.), *Proceedings of the 38th International Conference on Machine Learning, ICML 2021, 18-24 July 2021, Virtual Event*, volume 139 of *Proceedings of Machine Learning Research*, pp. 8748–8763. PMLR, 2021. URL <http://proceedings.mlr.press/v139/radford21a.html>.
- Benjamin Recht, Rebecca Roelofs, Ludwig Schmidt, and Vaishaal Shankar. Do ImageNet classifiers generalize to ImageNet? In *International Conference on Machine Learning*, pp. 5389–5400, 2019.
- Olga Russakovsky, Jia Deng, Hao Su, Jonathan Krause, Sanjeev Satheesh, Sean Ma, Zhiheng Huang, Andrej Karpathy, Aditya Khosla, Michael S. Bernstein, Alexander C. Berg, and Li Fei-Fei. Imagenet large scale visual recognition challenge. *CoRR*, abs/1409.0575, 2014. URL <http://arxiv.org/abs/1409.0575>.
- Christoph Schuhmann, Richard Vencu, Romain Beaumont, Robert Kaczmarczyk, Clayton Mullis, Aarush Katta, Theo Coombes, Jenia Jitsev, and Aran Komatsuzaki. LAION-400M: open dataset of clip-filtered 400 million image-text pairs. *CoRR*, abs/2111.02114, 2021. URL <https://arxiv.org/abs/2111.02114>.
- Candice Schumann, Susanna Ricco, Utsav Prabhu, Vittorio Ferrari, and Caroline Rebecca Pantofaru. A step toward more inclusive people annotations for fairness. In *Proceedings of the AAAI/ACM Conference on AI, Ethics, and Society (AIES)*, 2021.
- Oleksii Sidorov, Ronghang Hu, Marcus Rohrbach, and Amanpreet Singh. TextCaps: a dataset for image captioning with reading comprehension. In *European conference on computer vision*, pp. 742–758, 2020.
- Amanpreet Singh, Vivek Natarajan, Meet Shah, Yu Jiang, Xinlei Chen, Dhruv Batra, Devi Parikh, and Marcus Rohrbach. Towards VQA models that can read. In *Proceedings of the IEEE/CVF conference on computer vision and pattern recognition*, pp. 8317–8326, 2019.
- Yi Tay, Mostafa Dehghani, Vinh Q. Tran, Xavier Garcia, Jason Wei, Xuezhi Wang, Hyung Won Chung, Siamak Shakeri, Dara Bahri, Tal Schuster, Huaixiu Steven Zheng, Denny Zhou, Neil Houlsby, and Donald Metzler. UI2: Unifying language learning paradigms, 2023.
- Ashish V. Thapliyal, Jordi Pont-Tuset, Xi Chen, and Radu Soricut. Crossmodal-3600: A massively multilingual multimodal evaluation dataset. In *Conference on Empirical Methods in Natural Language Processing*, 2022.
- Michael Tschanen, Manoj Kumar, Andreas Steiner, Xiaohua Zhai, Neil Houlsby, and Lucas Beyer. Image captioners are scalable vision learners too. *CoRR*, abs/2306.07915, 2023. doi: 10.48550/arXiv.2306.07915. URL <https://doi.org/10.48550/arXiv.2306.07915>.
- Ashish Vaswani, Noam Shazeer, Niki Parmar, Jakob Uszkoreit, Llion Jones, Aidan N. Gomez, Lukasz Kaiser, and Illia Polosukhin. Attention is all you need. *CoRR*, abs/1706.03762, 2017. URL <http://arxiv.org/abs/1706.03762>.
- Bryan Wang, Gang Li, Xin Zhou, Zhourong Chen, Tovi Grossman, and Yang Li. Screen2words: Automatic mobile ui summarization with multimodal learning. In *The 34th Annual ACM Symposium on User Interface Software and Technology*, UIST ’21, pp. 498–510, New York, NY, USA, 2021a. Association for Computing Machinery. ISBN 9781450386357. doi: 10.1145/3472749.3474765. URL <https://doi.org/10.1145/3472749.3474765>.
- Jianfeng Wang, Zhengyuan Yang, Xiaowei Hu, Linjie Li, Kevin Lin, Zhe Gan, Zicheng Liu, Ce Liu, and Lijuan Wang. Git: A generative image-to-text transformer for vision and language. *arXiv preprint arXiv:2205.14100*, 2022a.
- Wenhui Wang, Hangbo Bao, Li Dong, Johan Bjorck, Zhiliang Peng, Qiang Liu, Kriti Aggarwal, Owais Khan Mohammed, Saksham Singhal, Subhojit Som, and Furu Wei. Image as a foreign language: Beit pretraining for all vision and vision-language tasks. *CoRR*, abs/2208.10442,

- 2022b. doi: 10.48550/arXiv.2208.10442. URL <https://doi.org/10.48550/arXiv.2208.10442>.
- Xin Wang, Jiawei Wu, Junkun Chen, Lei Li, Yuan-Fang Wang, and William Yang Wang. VateX: A large-scale, high-quality multilingual dataset for video-and-language research. In *Proceedings of the IEEE/CVF International Conference on Computer Vision*, pp. 4581–4591, 2019.
- Zirui Wang, Jiahui Yu, Adams Wei Yu, Zihang Dai, Yulia Tsvetkov, and Yuan Cao. SimVLM: Simple visual language model pretraining with weak supervision. *arXiv preprint arXiv:2108.10904*, 2021b.
- Junbin Xiao, Xindi Shang, Angela Yao, and Tat-Seng Chua. Next-qa: Next phase of question-answering to explaining temporal actions. In *Proceedings of the IEEE/CVF Conference on Computer Vision and Pattern Recognition*, pp. 9777–9786, 2021.
- Dejing Xu, Zhou Zhao, Jun Xiao, Fei Wu, Hanwang Zhang, Xiangnan He, and Yueting Zhuang. Video question answering via gradually refined attention over appearance and motion. In *Proceedings of the 25th ACM international conference on Multimedia*, pp. 1645–1653, 2017.
- Haiyang Xu, Qinghao Ye, Ming Yan, Yaya Shi, Jiabo Ye, Yuanhong Xu, Chenliang Li, Bin Bi, Qi Qian, Wei Wang, Guohai Xu, Ji Zhang, Songfang Huang, Fei Huang, and Jingren Zhou. mplug-2: A modularized multi-modal foundation model across text, image and video. In Andreas Krause, Emma Brunskill, Kyunghyun Cho, Barbara Engelhardt, Sivan Sabato, and Jonathan Scarlett (eds.), *International Conference on Machine Learning, ICML 2023, 23-29 July 2023, Honolulu, Hawaii, USA*, volume 202 of *Proceedings of Machine Learning Research*, pp. 38728–38748. PMLR, 2023. URL <https://proceedings.mlr.press/v202/xu23s.html>.
- Jun Xu, Tao Mei, Ting Yao, and Yong Rui. MSR-VTT: A large video description dataset for bridging video and language. In *Proceedings of the IEEE/CVF Conference on Computer Vision and Pattern Recognition*, 2016.
- Jiahui Yu, Zirui Wang, Vijay Vasudevan, Legg Yeung, Mojtaba Seyedhosseini, and Yonghui Wu. CoCa: Contrastive captioners are image-text foundation models. *arXiv preprint arXiv:2205.01917*, 2022.
- Licheng Yu, Patrick Poirson, Shan Yang, Alexander C Berg, and Tamara L Berg. Modeling context in referring expressions. In *Computer Vision—ECCV 2016: 14th European Conference, Amsterdam, The Netherlands, October 11-14, 2016, Proceedings, Part II 14*, pp. 69–85. Springer, 2016.
- Zhou Yu, Dejing Xu, Jun Yu, Ting Yu, Zhou Zhao, Yueting Zhuang, and Dacheng Tao. ActivityNet-qa: A dataset for understanding complex web videos via question answering. In *Proceedings of the AAAI Conference on Artificial Intelligence*, volume 33, pp. 9127–9134, 2019.
- Xiaohua Zhai, Alexander Kolesnikov, Neil Houlsby, and Lucas Beyer. Scaling vision transformers. In *Proceedings of the IEEE/CVF Conference on Computer Vision and Pattern Recognition*, pp. 12104–12113, 2022a.
- Xiaohua Zhai, Xiao Wang, Basil Mustafa, Andreas Steiner, Daniel Keysers, Alexander Kolesnikov, and Lucas Beyer. Lit: Zero-shot transfer with locked-image text tuning. In *IEEE/CVF Conference on Computer Vision and Pattern Recognition, CVPR 2022, New Orleans, LA, USA, June 18-24, 2022*, pp. 18102–18112. IEEE, 2022b. doi: 10.1109/CVPR52688.2022.01759. URL <https://doi.org/10.1109/CVPR52688.2022.01759>.
- Xiaohua Zhai, Basil Mustafa, Alexander Kolesnikov, and Lucas Beyer. Sigmoid loss for language image pre-training. In *International Conference on Computer Vision*, 2023.
- Zijia Zhao, Longteng Guo, Tongtian Yue, Sihan Chen, Shuai Shao, Xinxin Zhu, Zehuan Yuan, and Jing Liu. Chatbridge: Bridging modalities with large language model as a language catalyst. *CoRR*, abs/2305.16103, 2023. doi: 10.48550/arXiv.2305.16103. URL <https://doi.org/10.48550/arXiv.2305.16103>.

A ADDITIONAL RESULTS: VIDEO CAPTIONING AND QA

A.1 DATASETS & BENCHMARKS

Because not all videos in the benchmarks are available online at the time of experimentation when freshly collected the data, the effective numbers of videos is smaller than the public official splits in some cases. Table 10 reports the details numbers for the subset used in our training and evaluation. We follows the same experimental settings used in PaLI-X (Chen et al., 2023a), including the dataset splits configuration and the evaluation metrics. Please refer to PaLI-X (Chen et al., 2023a) for more data-related details.

		MSR-VTT	VATEX	ANet-Cap	SMIT	M-V-QA	ANet-QA	NExT-QA
Original size	valid.	497	3000	17505	14604	12278	18000	5343
	test	2990	6000	17031	3513	72821	8000	9178
Dataset size	valid.	325	2646	14566	8096	8160	10000	5343
	test	2135	5242	14197	3513	52623	7040	9178
% Remaining	valid.	65.39	88.20	83.21	100.00	66.46	-	100.00
	test	71.40	87.37	83.36	100.00	72.26	88.00	100.00

Table 10: As we freshly collect the data sets, the actual amount of training data is smaller than the public benchmarks, making the tasks more challenging. Except for NextQA and SMIT, there are more than 10% of the videos missing in both training and evaluation.

B ADDITIONAL RESULTS: CROSSMODAL-3600 RETRIEVAL

We present more results of zero-shot image-text retrieval results (recall@1) on Crossmodal-3600 (Thapliyal et al., 2022) in this section. Detailed results across 36 languages for SigLIP ViT-G and Classif ViT-e are presented in Figure 3, Figure 4 and Table 11.

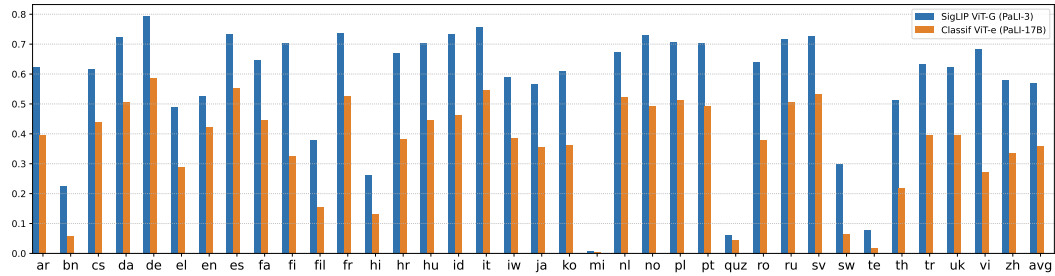


Figure 3: Image-to-text zero-shot retrieval recall@1 on crossmodal-3600 for SigLIP ViT-G and Classif ViT-e.

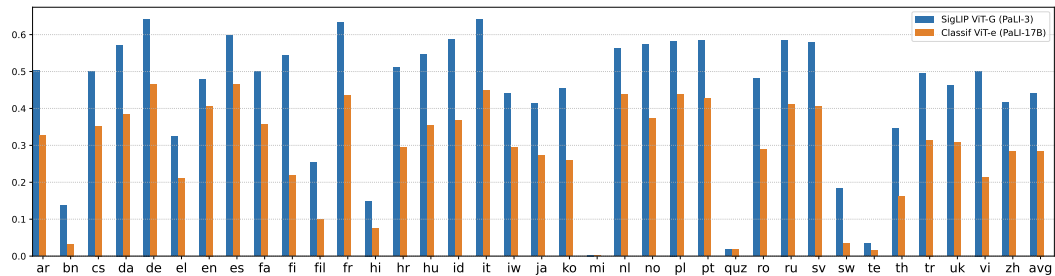


Figure 4: Text-to-image zero-shot retrieval recall@1 on crossmodal-3600 for SigLIP ViT-G and Classif ViT-e.

Language	Image-to-text		Text-to-image	
	SigLIP ViT-G	Classif ViT-e	SigLIP ViT-G	Classif ViT-e
ar	62.22	39.69	50.33	32.60
bn	22.67	5.67	13.61	3.31
cs	61.69	44.03	50.10	35.24
da	72.47	50.75	57.16	38.48
de	79.28	58.53	64.20	46.50
el	49.11	29.03	32.36	20.92
en	52.64	42.11	47.89	40.63
es	73.31	55.22	59.77	46.55
fa	64.56	44.50	50.09	35.58
fi	70.39	32.64	54.34	21.80
fil	37.89	15.53	25.40	10.04
fr	73.81	52.61	63.28	43.47
hi	26.22	13.14	14.94	7.42
hr	66.89	38.31	51.03	29.55
hu	70.22	44.67	54.63	35.49
id	73.53	46.33	58.62	36.75
it	75.56	54.53	64.14	44.76
iw	59.14	38.67	44.10	29.39
ja	56.69	35.47	41.31	27.24
ko	61.03	36.11	45.50	25.95
mi	0.64	0.33	0.30	0.22
nl	67.25	52.14	56.23	43.79
no	73.03	49.17	57.40	37.35
pl	70.69	51.42	58.24	43.72
pt	70.22	49.19	58.47	42.73
quz	6.28	4.31	1.89	1.90
ro	63.92	37.75	48.20	28.82
ru	71.69	50.64	58.51	41.11
sv	72.69	53.22	57.76	40.66
sw	29.86	6.42	18.31	3.41
te	7.81	1.92	3.39	1.42
th	51.14	22.00	34.65	16.06
tr	63.36	39.50	49.41	31.47
uk	62.19	39.53	46.15	30.81
vi	68.50	27.08	50.14	21.28
zh	57.92	33.61	41.51	28.24
avg	56.85	35.99	43.98	28.46

Table 11: Crossmodal-3600 zero-shot retrieval recall@1 (%) for SigLIP ViT-G (2B params) and Classif ViT-e (4B params). SigLIP ViT-G is significantly better than Classif ViT-e across all the languages. SigLIP improves from 28.5% to 44.0% on average for the text-to-image retrieval task.